Robust Range Image Registration using Local Distribution of Albedo

Diego Thomas
National Institute of Informatics
Tokyo 101-8430, Japan
diego_thomas@nii.ac.jp

Akihiro Sugimoto
National Institute of Informatics
Tokyo 101-8430, Japan
sugimoto@nii.ac.jp

Abstract

We propose a robust registration method for range images under a rough estimate of illumination. Because reflectance properties are invariant to changes in illumination, they are promising to range image registration of objects lacking in discriminative geometric features under variable illumination. In our method, we use adaptive regions to model the local distribution of reflectance, which enables us to stably extract reliable attributes of each point against illumination estimation. We use a level set method to grow robust and adaptive regions to define these attributes. A similarity metric between two attributes is defined using the principal component analysis to find matches. Moreover, remaining mismatches are efficiently removed using the rigidity constraint of surfaces. Our experiments using synthetic and real data demonstrate the robustness and effectiveness of our proposed method.

1. Introduction

The 3D modeling process of real objects has attracted growing interest during the past decade for applications in augmented reality, cinema, computer games or medicine. Because creating the detailed 3D model of a real object using some modeling software is labour intensive, automating the whole modeling process has attracted substantial interest in recent years. This process can be divided in five steps: (1) data acquisition, (2) reconstruction of 3D images, (3) 3D registration, (4) merging and (5) inverse rendering.

Recent acquisition devices, like a modern laser range scanner, can retrieve both the 3D shape and a color image of an object from a fixed viewpoint, the acquired 3D image in this case is called a range image. Therefore, for the case of range images, the second step of the 3D modeling process can be omitted. However, as from a fixed viewpoint some parts of the object are occluded, multiple viewpoints are thus required to obtain the full 3D shape of the object. Therefore, partially overlapping parts of the object, acquired from different viewpoints have to be aligned. This process is called 3D registration. Two categories exist for 3D registration. The first one, called coarse registration, is to find a rough alignment between two 3D images, starting from sufficiently different poses. The second one, called fine registration, is to find accurate alignment between two 3D images, starting from a rough alignment. When using range images, we refer as range image registration.

The most famous approach to fine registration is ICP (Iterative Closest Point) [2]. This method iterates two steps: matching of each point of the first image with its closest point on the other image; estimation of the transformation between the two images using the matched point correspondences. ICP converges with a local estimate and therefore requires a rough alignment for initialization. To achieve robust and accurate alignment, many discriminative geometric features have been proposed ([11], [7], [1], [8]).

To overcome the problem of objects devoid of salient geometric features, many approaches using photometric features have been also discussed. Godin *et al.* [5] proposed to use dense attributes of range image elements as a matching constraint. Weik [14] proposed to use texture intensity gradient and intensity difference. Johnson and Kang [9] proposed to deal with textured 3D shapes by using color. Okatani *et al.* [12] proposed to use chromaticity for registration. Brusco *et al.* [3] proposed to incorporate texture information in the concept of spin-images. Pulli *et al.* [13] proposed a new mismatch error to improve registration using both color and geometric information.

One difficulty in directly using color or chromaticity for registration is its dependence on the measuring conditions such as distance, orientation or illumination conditions. Most of the time the color consistency assumption is not verified. Recently, Cerman *et al.* [4] proposed a method, which we call ICPA (ICP using Albedo), using reflectance properties (which is the albedo for the case of Lambertian objects) of the object surface into the ICP process.

Reflectance properties are promising because of their independence to the object pose relative to the sensor. Retrieving these properties has provided a major research area in physics-based vision called reflectance from brightness (with a known shape and illumination). In order to re-

2009 IEEE 12th International Conference on Computer Vision Workshops, ICCV Workshops
978-1-4244-4441-0/09/$25.00 ©2009 IEEE

trieve accurate reflectance of the surface of an object from its shape and brightness, the illumination conditions have to be precisely known a priori. As a consequence, a direct use of albedo values as a matching constraint, as proposed in ICPA, requires a precise estimate of global illumination which is practically difficult to obtain in the case of real illumination conditions.

We introduce a region-based approach to using reflectance attributes for robust fine registration of Lambertian objects under rough estimation of illumination. Because retrieving reflectance attributes on the surface of a Lambertian object (which is the albedo in this case) is sensitive to illumination estimation, direct use of albedo of a point is not effective under rough illumination estimation. We thus employ the local distribution of albedo for registration. Our proposed method uses adaptive regions to model the local distribution of albedo on the object surface, which leads to robust attribute extraction against illumination estimations. These regions are grown using a level set method, allowing us to exclude many outliers and then to define more reliable attributes. We define a robust metric, using the PCA (Principal Component Analysis) of each region to find point correspondences. This is a stable and powerful metric to maximize the number of correct matching, even under rough illumination estimation. Moreover, enforcing the rigidity constraint on surfaces, we reject remaining mismatching and then estimate the transformation using the weighted least square method. Our method has the advantage under rough estimation of illumination and under a large amount of noise. This advantage allows us to use simple illumination models for the registration of range images. Our experiments using synthetic and real data demonstrate the robustness of our method.

2. Proposed method

The registration process is carried out in an iterative manner by successively estimating the rigid transformation, until a convergence criterion is satisfied or a maximum of iterations is achieved. Matches are obtained by evaluating the similarities between reliable attributes of each points. These attributes are defined by adaptive regions representing the local distribution of albedo on the object surfaces. The transformation is then estimated by minimizing the distances between matched points.

2.1. Adaptive region generation

We define a region for each point of the range image to obtain reliable attributes of each point for finding point correspondences. The main idea here is to obtain a reliable representation of the local distribution of albedo. Therefore, these regions should be defined adaptively depending on the local distribution of albedo around the point of interest. Level set methods, which are widely used for segmentation, appear to be efficient to model complex shapes in textured images and are robust to data noise. Therefore, we adaptively grow regions using a level-set method.

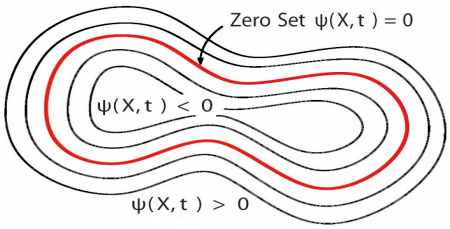

Figure 1: Concept of zero set in a level set.

2.1.1 Level set method

A region is defined by a contour. We define the contour with a level-set method (the fast marching algorithm [6]). A contour is defined as the zero level set of a higher dimensional function called the level-set function, $\psi(X,t)$ (see Fig. 1). The level-set function is then evolved under the control of a differential equation. At any time, the evolving contour can be obtained by extracting the zero level-set $\Gamma(t) = \{X \mid \psi(X,t) = 0\}$.

We use a simple form of the level-set equation:

$$\frac{d}{dt}\psi = -P(x)\|\nabla\psi\|, \tag{1}$$

where P is a propagation (expansion) term. This propagation term of the level-set function will be defined in terms of a speed image.

The speed image. The speed image represents how fast a contour can propagate for every point of the range image. This speed should depends on the homogeneity of the albedo of every point compared with their local neighborhood. In the proposed method, the speed image is computed as a function of the gradient magnitude image of albedo, computed using the Gradient Magnitude filter. The mapping should be done in such a way that the propagation speed of the front is very low with high albedo gradients while it becomes rather fast in low gradient areas. This arrangement makes the contour propagate until it reaches the edges of albedo patterns and then slow down in front of those edges.

We employ the Sigmoid function S to compute the speed image since it offers a good deal of control parameters that can be customized to shape a nice speed image. In fact, it has a mechanism for focusing attention on a particular set of values and progressively attenuating the values outside that range.

$$S(I) = \frac{1}{1 + e^{-(\frac{I-\beta}{\alpha})}}, \tag{2}$$

where I is the gradient image of albedo, α defines the width of the gradient intensity range, and β defines the gradient

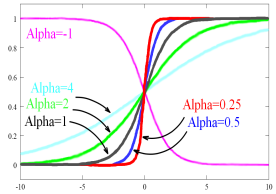

(a) α defines the width of the window.

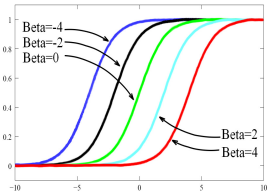

(b) β defines the center of the window.

Figure 2: Effects of the various parameters in the Sigmoid function.

intensity around which the range is centered (see Fig. 2). As suggested in [6], α and β are found as follows. For the gradient magnitude image, let us denote by $K1$ the minimum value along the contour of the albedo patterns. We denote by $K2$ the average value of the gradient magnitude in the homogeneous regions of the albedo image. Then, β is $\frac{K1+K2}{2}$ while α is $\frac{K2-K1}{6}$.

2.1.2 Region generation

For each point p, we define a time image T_p. For each pixel x of T_p, $T_p(x)$ represents the time required for the level-set function to propagate from p to x. Starting from a point p, a region is grown by using the 4-neighbourhood and by adding into the region, points such that T_p on these points is less than a threshold (for example 0.2 seconds) (see Fig. 3). A maximum size of the region is enforced, which will allow us to discriminate points in too homogeneous areas.

This region grows in homogeneous areas and stops in front of the contour of albedo patterns. Consequently, while the size of the region increases, the homogeneity of the region is preserved. Moreover, the growth of the region is adapted to the distribution of albedo and to data noise in the neighborhood of each point. As a result, a reliable region is adaptively generated depending on each point. The local distribution of albedo of 3D points inside this region defines an attribute for each point. The attributes obtained in this way enhance robustness in evaluating similarity to find correspondences.

2.2. Restriction of the searching area

Under a rough estimate of illumination, the estimation of albedo becomes poor. In particular, it will be far useless around the border of the range image. Consequently, in order to reduce the influence arising around the border, we do not consider points near the borders of the range image. We denote by $C(P)$ the restricted area of the range image P.

Moreover, we dynamically control for each point $p \in P$ a searching area (the area where a possible match of p is searched) $\Omega(p)$ in the range image Q, whose center is the projection of p on Q. $\Omega(p)$ is defined such that the closer to convergence the registration becomes, the smaller $\Omega(p)$ becomes. This control enhances stability and accuracy of registration. $\Omega(p)$ is defined independently of $C(Q)$.

Points in large homogeneous areas are not discriminative enough to be used in the registration. Such points are detected using the size of their regions. Indeed, region sizes of such points are close to the maximum size given beforehand. Therefore we do not consider points whose region size is greater than 95% of the maximum size of regions.

2.3. Similarity evaluation using albedo

Using the attribute of a point, we define a similarity metric between two points to find correspondences across two range images.

Letting p be a point in $C(P)$ and q be a point in $\Omega(p)$, we define $R(p)$ and $R(q)$ as the regions corresponding to p and q. We then apply PCA (Principal Component Analysis) to $R(p)$ and $R(q)$ to find the transformation T that aligns the three principal axis of $R(p)$ to those of $R(q)$. For each point $m \in R(p)$, we define its corresponding point $n(m)_q \in R(q)$ (Fig. 4). The corresponding point $n(m)_q$ is defined by

$$\arg \min_{x \in R(q)} (\|T(\overrightarrow{pm}) - \overrightarrow{qx})\|_2). \tag{3}$$

For each pair $(m, n(m)_q)$ we define a weight $\omega_{(m,q)}$ such as

$$\begin{aligned} \omega_{(m,q)} &= 0 \text{ if } \|T(\overrightarrow{pm}) - \overrightarrow{qn(m)_q})\|_2 > thresh, \\ \omega_{(m,q)} &= 1 \text{ if } \|T(\overrightarrow{pm}) - \overrightarrow{qn(m)_q})\|_2 \leq thresh, \end{aligned} \tag{4}$$

where $thresh$ is a distance threshold (for example 0.4mm). In the similar way, we can define the corresponding point and weight for each point in $R(q)$.

The similarity function between two points p and q is then defined as the weighted sum of the differences of albedo of the corresponding pairs:

$$\begin{aligned} L(p,q) = & \frac{size(R(p)) + size(R(q))}{(\sum_{m \in R(p)} \omega_{(m,q)} + \sum_{m \in R(q)} \omega_{(m,p)})^2} \\ & \times \Big\{ \sum_{m \in R(p)} \omega_{(m,q)} \|\overrightarrow{alb(m)} - \overrightarrow{alb(n(m)_q)}\|_2^2 \\ & + \sum_{m \in R(q)} \omega_{(m,p)} \|\overrightarrow{alb(m)} - \overrightarrow{alb(n(m)_p)}\|_2^2 \Big\}, \end{aligned} \tag{5}$$

where $size(R(\cdot))$ is the number of points in $R(\cdot)$ and $\overrightarrow{alb(m)}$ is the albedo vector of point m, computed using the Lambertian model of reflectance for each color channel:

$$\overrightarrow{alb(m)} = \frac{\overrightarrow{c(m)}}{\overrightarrow{n(m)}^\top M \overrightarrow{n(m)}}, \tag{6}$$

where $\overrightarrow{n(m)}$ is the normal of the surface at point m, M is the illumination matrix and $\overrightarrow{c(m)}$ is the RGB vector of point m.

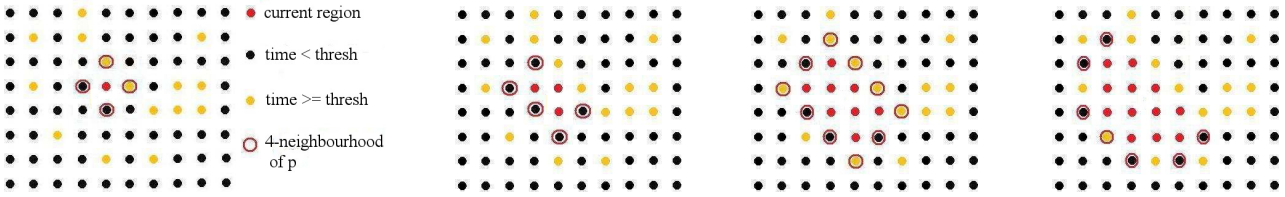

(a) Initial state. (b) First step. (c) Second step. (d) Third step.

Figure 3: Adaptively defined region using a 4-neighbourhood.

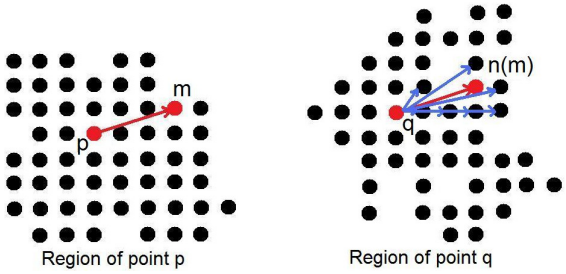

Figure 4: Searching for the corresponding point of m.

If p and q are matches and two regions $R(p)$ and $R(q)$ represent the same part of the object viewed from different viewpoints, then $m \in R(p)$ and $n(m)_q \in R(q)$ will represent the same point viewed from different viewpoints. Thus, their albedo will be similar. Therefore, the function L becomes small for points p and q. To the contrary, L becomes large for points having different regions. As we see, supports by the corresponding points inside the region define the similarity between two points of interest. This leads to robust and stable evaluation of similarity.

We note that if $\sum_{m \in R(p)} \omega_{(m,q)}$ or $\sum_{m \in R(q)} \omega_{(m,p)}$ is less than $0.6 \times size(R(p))$, *resp.* $0.6 \times size(R(q))$, then the pair (p, q) is not considered as a possible match. This is because if (p, q) is a correct match, we can expect that a sufficient number of matches exists between $R(p)$ and $R(q)$.

At the end of this step, we have a reliable list of matches that does not contain any isolated points. Indeed, the region grown from an isolated point is empty and thus, this point will not be a candidate for any match.

2.4. Incorrect matches elimination

The obtained list of matches cannot be always directly used as an input of the transformation estimation step. This is because a large amount of noise or repetitive patterns in albedo distribution may cause incorrect matches. We here remove such incorrect matches in order to enhance the robustness of the transformation estimation further. To evaluate the correctness of matches, we use the rigidity constraint of surfaces. This is because the rigidity constraint does not depend on intensity or normals and thus it is robust against data noise.

For two corresponding pairs (p, q), (p', q') in the range images P and Q, we consider point pairs (p, p') and (q, q') which represent the same points viewed from different viewpoints. Assuming that surfaces are rigid, we see that the distances $\|\overrightarrow{pp'}\|_2$ and $\|\overrightarrow{qq'}\|_2$ should not be too different from each other. Namely, we define d representing the difference between $\|\overrightarrow{pp'}\|_2$ and $\|\overrightarrow{qq'}\|_2$:

$$d = |\|\overrightarrow{pp'}\|_2 - \|\overrightarrow{qq'}\|_2|. \tag{7}$$

If (p, q) and (p', q') are correct matches, then d should be smaller than a threshold $Tdist$ ($1.0\mathrm{mm}$ for a resolution of $0.55\mathrm{mm}$ for example). This gives us the rigidity constraint (see Fig. 5).

Each pair in the list of matches is evaluated with all the other pairs in the list. If the number of pairs that violates the rigidity constraint exceeds a certain percentage $Perc$ (50% for example) of the pairs, then the current pair is considered as an incorrect match and removed from the list.

Assuming that the majority of the obtained pairs are correct matches, this method efficiently removes incorrect matches from the list of pairs obtain in Section 2.3. In order to handle the case where the majority of matches are incorrect, we dynamically update the parameters $Tdist$ and $Perc$ in such a way that the elimination step is tolerant to mismatches at the beginning of the registration, and strict to mismatches at the end of the registration. This is because, in the beginning of the registration we may have a large amount of mismatches and only a rough estimate of the transformation is sufficient. In contrast, as the registration becomes accurate, there are less mismatches and we aim at eliminating as many mismatches as possible to refine the estimation of the transformation.

Our outlier elimination approach is simpler than the RANSAC method while its computational complexity ($\mathrm{O}(n^2)$) remains low where n is the number of matches in the list.

2.5. Transformation estimation

In order to estimate the transformation as accurately as possible, we use the WLS method [10]. This method weights each pair with the Euclidean distance between the two corresponding points during the least square minimiza-

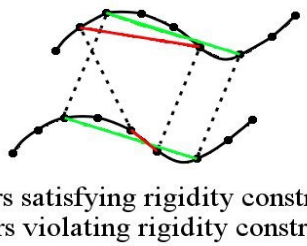

Figure 5: Principle of the rigidity constraint.

tion. These weights represent the feasibility of the correspondence of paired points. The minimization is iteratively performed with updating the weight of each pair. The resulting transformation obtained with this method is more accurate than that with the standard least squared method.

3. Experiments

We evaluated our method using synthetic and real data and compared with ICPA and ICP using both chromaticity and geometric features (which we call ICP-CG). We note that the restriction of the searching area in Section 2.2 was applied to the three methods equivalently.

3.1. Definition of parameters

The three methods have several parameters to be fixed. ICPA and ICP-CG require three parameters: max_it, the maximum of iterations for the registration; $conv\_thresh$, the threshold for convergence and $percentage$, the percentage of matches to be eliminated.

Our proposed method requires four parameters:max_it; $conv\_thresh$; $thresh$, the threshold to grow the regions and max_size, the maximum size of a region. For the elimination step, the two thresholds $Tdist$ and $Perc$ are dynamically defined depending on the current state of the registration. At the beginning of the registration, $Tdist = 8\times$"resolution of the image" and $Perc = 70\%$; at the end of the registration, $Tdist = 2\times$"resolution of the image" and $Perc = 30\%$.

3.2. Evaluation with synthetic data

We conducted experiments with synthetic data to test the robustness of the proposed method against changes in illumination. The synthetic data were obtained with a 3D modeler software (3D Studio Max) (see Table 1). The exact albedo image and the exact illumination, which correspond to a spot light, are known. Assuming the object to be Lambertian, we simulated color with an estimation of the exact illumination to test the robustness of our proposed method (see Fig. 6).

In order to see the effects against estimated illumination, we transformed the exact illumination matrix by a rotation $R(\theta)$. $R(\theta)$ is the composition of three particular rotations around the three axes x, y, z. The three rotation angles for the rotation around each axis were independently sampled from the uniform distribution of $[-\theta, \theta]$

Before applying our method, we manually established a rough pre-alignment of the two range images. This alignment allowed us to simulate the case where the input data were captured from two viewpoints rotationally differentiated by 17.93 degrees around the axis $(0.0076, -0.9995, 0.0319)$. We used the same sets of parameters for all synthetic experiments: $max\_it = 10$; $conv_thresh = 0.02$radian; for ICPA, $percentage = 30\%$; for the proposed method, $thresh = 0.05$sec, $max_size = 0.1$mm.

We evaluated our method with different values of θ, and thus different estimations of the illumination. The value θ was changed from 0 to 54 degrees by 2.86 degrees (54 degrees correspond approximately to 0.95 radian and 2.86 degrees correspond approximately to 0.05 radian). For each values of θ, we applied our method 50 times under the same initial conditions.

Fig. 7 shows quantitative evaluation of registration results in terms of averages and variances of the angle error and axis error of the obtained results under various different estimations of illumination. As a comparison, the results obtained by ICPA are also shown. Since ICP-CG failed in the registration because of geometrical symmetries of the shape of the object, we did not perform comparative experiments with ICP-CG. As expected, we observe that our method is in average more accurate than ICPA and more stable for the estimation of the rotation angle and rotation axis. Results obtained with ICPA become inaccurate and unstable as soon as the estimated illumination slightly differs from the exact one (for θ greater than 6 degrees). With ICPA, the results are largely unsatisfactory when the illumination estimation is not close to the exact one. On the contrary, our proposed method obtained satisfactory results for θ up to 45 degrees. Therefore, we can conclude that our method is more robust to changes in illumination than ICPA. Moreover, for exact illumination estimation, our proposed method achieved registration as accurate as ICPA.

Fig. 8 shows an example of quantitative results of registration obtained with our proposed method under various noise levels of intensities where the estimated illumination corresponds to $\theta = 8.6$ degrees. We applied a Gaussian noise with variance of several percentages of the average of the image intensities. For each different level of noise we applied our method 50 times under the same initial conditions. We observe that even with a noise of variance 16%, the largest errors are under 0.2 degree for the angle accuracy and under 3 degrees for the axis accuracy.

We also performed intensive experiments under noise added to normals and we obtained similar behavior of errors. From these results, we observe that our method is sta-

Table 1: Description of the synthetic data.

Nb_Points	Resolution	Expected_rot (angle; axis)
30650	0.01mm	$(17.93; 0.0076, -0.9995, 0.0319)$

(a) First image. (b) Second image. (c) Albedo image.

Figure 6: The input synthetic data.

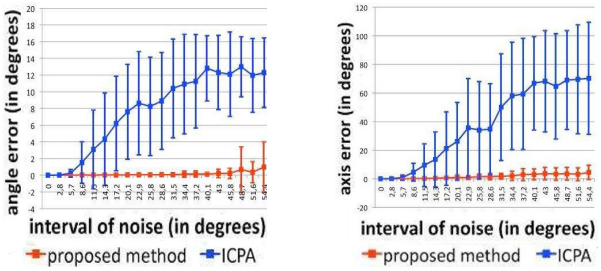

(a) Angle error. (b) Axis error.

Figure 7: Results under various different illuminations.

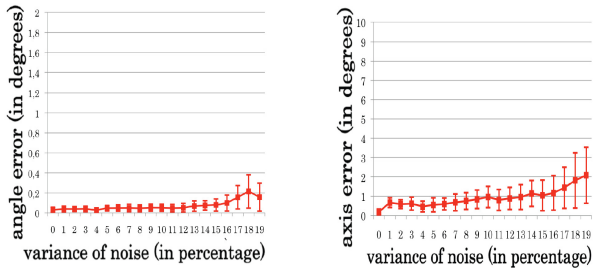

(a) Angle error. (b) Axis error.

Figure 8: Results under noise in intensities with our method.

ble against geometric and photometric noise.

3.3. Evaluation with real data

We conducted experiments using real objects to test the effectiveness of the proposed method. We employed a Konica Minolta Vivid 910 range scanner, which captures the 3D shape and the texture of an object. A mechanic system was used to rotate the object and acquire ground truth of rotation.

The proposed method starts with an estimate of the geometric transformation and with a rough estimate of global illumination conditions to estimate albedo. The initial estimation of registration is obtained by just superimposing the two captured range images. The global illumination is manually estimated in a rough manner by rotating and scaling an illumination matrix, which corresponds to a spot light. This explains the greenish aspect observed in the albedo images in Fig.10(a) and Fig.14. We used the same sets of parameters for all experiments: $max\_it = 15$; $conv\_thresh = 0.002\text{radian}$; for ICP-CG and ICPA, $percentage = 30\%$; for the proposed method, $thresh = 0.2\text{sec}$, $max\_size = 5.5\text{mm}$. This means that we need not extra tuning of the parameters depending on objects.

(a) First image. (b) Second image. (c) Superimposed.

Figure 9: Range images captured from different viewpoints.

(a) Albedo image. (b) Gradient map. (c) Speed map.

Figure 10: Illumination conditions and region generation.

We obtained two range images of a can that has a height of about 10cm and a diameter of about 5cm and was rotationally symmetric (Fig.9). Fig. 10 shows the gradient image and the speed image computed from the albedo estimation. In order to demonstrate the effectiveness of our method, we compared the results obtained by ICPA and ICP-CG (Figs. 11 and 12). We note that the same initial estimation was used for the three methods. Details on data are shown in Table 2 and quantitative results are shown in Table 3. In these tables, Nb_Points is the number of points in the range image; Res is the resolution of the range image; $NbIt$ represents the number of iterations required to achieve convergence; $NbMPts$ represents the number of matched points at the end of the registration; $Final\_rot$ is the estimated rotation after registration; $Angle\_Error$ represents the difference between the expected rotation angle and the obtained one and $Axis\_Error$ represents the angle between the expected rotation axis and the obtained one.

Because of the lack of geometric features, ICP-CG failed in registering the two range images. The registration result obtained with ICPA, although it is more accurate than ICP-

Table 3: Quantitative evaluation of the registration, using data can.

	NbIt	NbMPts	Final_rot (angle; axis)	Angle_Error	Axis_Error
Proposed Method	14	3400	(19.780; -0.009, -0.949, -0.316)	0.22deg	1.87deg
ICPA	15	11700	(12.580; 0.030, -0.998, 0.057)	7.42deg	23.70deg
ICP-CG	10	11800	(3.740; -0.010, -0.996, -0.086)	16.26deg	15.31deg

Figure 11: From left to right, results obtained with our method, ICPA and ICP-CG.

Figure 12: From left to right, zoom on the above square part of the results obtained with our method, ICPA and ICP-CG.

Table 2: Description of data can used for the experiment.

Nb_Points	Res	Expected_rot (angle; axis)
25000	0.55mm	(20.00; −0.010, −0.930, −0.340)

Table 4: Description of data hand and box.

	Nb_Points	Res	Expected_rot (angle; axis)
hand	50000	0.55mm	(20.020; 0.040, −0.940, −0.320)
box	90000	0.55mm	(20.000; 0.000, −0.940, −0.320)

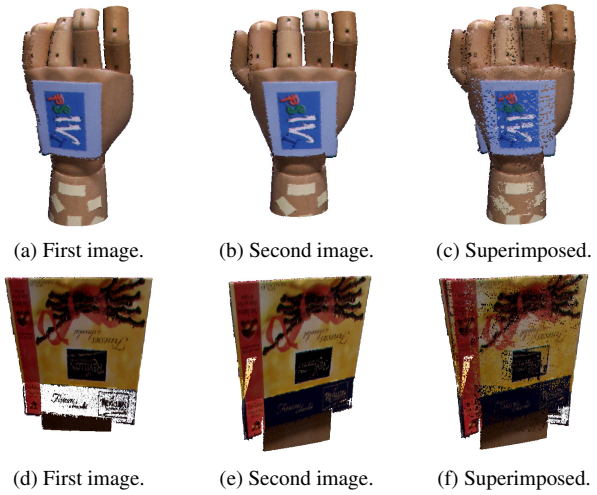

(a) First image. (b) Second image. (c) Superimposed.

(d) First image. (e) Second image. (f) Superimposed.

Figure 13: Initial state for data *hand* (top) and *box* (bottom).

CG, is not satisfactory. In contrast, we can see significant improvements in the registration obtained with the proposed method. We remark that 15% of matched pairs were eliminated as incorrect matches in our method. When the searching area (see Section 2.2) was not dynamically restricted by $\Omega(\cdot)$, the results obtained with the three methods were less accurate. Indeed, in this case, the angle errors were 4.00, 12.58 and 16.40 degrees while the axis errors were 1.60, 19.00 and 12.00 degrees with our proposed method, ICPA and ICP-CG respectively.

Fig. 15 shows results obtain with different objects called hand and box. Table 4 shows a description of each data before registration. We note that the hand (resp. the box) has a height of about 20cm (resp. 10cm) and a width of about 10cm (resp. 20cm). Figs. 13 and 14 show initial estimation of registration and global illumination. Fig. 15 shows comparison of the results by our method, ICPA and ICP-CG. Quantitative results of these experiments are shown in Table 5. Identified incorrect matches were 35% for hand data and 7% for box data. The average of computational time required for the registration of these images was about 10minutes with an Intel Core 2 Duo CPU 3GHz.

Because of the lack of discriminative geometric features, methods using only geometric features are not sufficient. Moreover, because of changes in color due to illumination, color information like chromaticity can not be used directly. In fact, both ICPA and ICP-CG did not have satisfactory results due to data noise and inaccurate estimation of illumination. Our method succeeded in registration of range images with an accuracy around the resolution of the range sensor for all data.

4. Conclusion

We introduced a region-based range image registration using reflectance attributes under rough illumination condition estimations. Our method stably extracts reliable attributes that capture local albedo distribution on the object surface. These attributes are defined by adaptively growing regions generated using a level set method. Such attributes are used to evaluate the similarity of points to ob-

Table 5: Quantitative evaluation of registrations, using data hand and box.

		NbIt	NbMPts	Final_rot (angle; axis)	Angle_Error	Axis_Error
hand	Proposed Method	15	7200	(20.070; -0.014, -0.946, -0.320)	0.05deg	3.63deg
hand	ICPA	15	25000	(19.420; -0.015, -0.919, -0.394)	0.60deg	5.80deg
hand	ICP-CG	15	25600	(19.190; -0.003, -0.945, -0.326)	0.83deg	4.58deg
box	Proposed Method	12	8500	$(20.010; -0.021, -0.945, -0.326)$	0.01deg	1.23deg
box	ICPA	15	38000	$(19.970; -0.030, -0.902, -0.387)$	0.03deg	4.40deg
box	ICP-CG	15	39120	$(19.94; -0.037, -0.880, -0.456)$	0.06deg	8.59deg

(a) Albedo image. (b) Albedo image.

Figure 14: Initial illumination state for data hand (left) and box (right).

Figure 15: From top to bottom, results obtained with the data hand and box. From left to right, results obtained with our method, ICPA and ICP-CG.

tain point correspondences robustly even under rough estimation of illumination conditions. Our method also efficiently removes mismatches by using the rigidity constraint of surfaces, which enhances the robustness of the registration process. Our experiments using synthetic and real data showed the improvements in robustness and accuracy of the registration results under rough estimation of illumination.

References

[1] S. Belongie, J. Malik, and J. Puzicha. Shape matching and object recognition using shape contexts. *IEEE Trans. on PAMI*, 24(4):509–522, 2002.

[2] P. J. Besl and N. D. McKay. A method for registration of 3-D shapes. *IEEE Trans. on PAMI*, 14(2):239–256, 1992.

[3] N. Brusco, M. Andreetto, A. Giorgi, and G. M. Cortelazzo. 3D registration by textured spin-images. *In Proc. of 3DIM'05*, pages 262–269, 2005.

[4] L. Cerman, A. Sugimoto, and I. Shimizu. 3D shape registration with estimating illumination and photometric properties of a convex object. *In Proc. of CVWW'07*, pages 76–81, 2007.

[5] G. Godin, D. Laurendeau, and R. Bergevin. A method for the registration of attributed range images. *In Proc. of 3DIM'01*, pages 179–186, 2001.

[6] L. Ibanez, W. Schroeder, L. Ng, j. Cates, and the Insight Software Consortium. The ITK software guide second edition. *The ITK Software Guide Second Edition*, 2005.

[7] B. Jian and B. C. Vemuri. A robust algorithm for point set registration using mixture of gaussian. *In Proc. of ICCV'05*, 2:1246–1251, 2005.

[8] A. E. Johnson and M. Hebert. Surface registration by matching oriented points. *In Proc. of 3DIM'97*, pages 121–128, 1997.

[9] A. E. Johnson and S. B. Kang. Registration and integration of textured 3D data. *Image and vision computing*, 17(2):135–147, 1999.

[10] Y. Liu, h. Zhou, X. Su, M. Ni, and R. J.Lloyd. Transforming least squares to weighted least squares for accurate range image registration. *In Proc. of 3DPVT'06*, pages 232–239, 2006.

[11] V.-D. Nguyen, V. Nzomigni, and C. V. Stewart. Fast and robust registration of 3D surfaces using low curvature patches. *In Proc. of 3DIM'99*, pages 201–208, 1999.

[12] Okatani, I.S., and A. Sugimoto. Registration of range images that preserves local surface structures and color. *In Proc. of 3DPVT'04*, pages 786–796, 2004.

[13] K. Pulli, S. Piiroinen, T. Duchamp, and W. Stuetzle. Projective surface matching of colored 3D scans. *In Proc. of 3DIM05*, pages 531–538, 2005.

[14] S. Weik. Registration of 3-D partial surface models using luminance and depth information. *In Proc. of 3DIM'97*, pages 93–101, 1997.